REGISTRATION AND RESTORATION OF ADAPTIVE-OPTICS CORRECTED RETINAL IMAGES.

A. Leonardo Blanco, B. Laurent M. Mugnier, C. Aurélie Montmerle Bonnefois, D. Michel Paques

A-C: ONERA – The French Aerospace Lab
Optics Department
29 av. Division Leclerc, BP 72, 92322 Châtillon cedex, France
D: Centre Hospitalier National d'Ophtalmologie des Quinze-Vingts
Centre d'Investigations Cliniques
28, rue de Charenton, 75 571 PARIS Cedex 12, France

ABSTRACT

Raw individual Adaptive-Optics-corrected flood-illuminated retinal images are usually quite noisy because of safety flux limitations. These flood-illuminated images are also of poor contrast. Interpretation of such images is therefore difficult without an appropriate post-processing, which typically includes the registration of the recorded image stack into a mosaic image and the restoration of the latter.

We have developed an image registration method in a MAP framework, based on previous work in astronomical imaging, and tailored for the specifics of retinal imaging, more precisely to the fact that the illumination of the retina and the transmission of the instrument is non-homogeneous, which makes conventional registration methods likely to fail.

The mosaic image must then be deconvolved in order to visually restore the high-resolution brought by adaptive optics. To this aim, we perform an unsupervised myopic deconvolution that takes into account the 3D nature of the object being imaged.

We successfully apply this whole processing chain to experimental in vivo images of retinal vessels.

1. INTRODUCTION

Adaptive Optics (AO) is a widespread technique improving the lateral resolution of retinal images – see [1] (this conference) for a review of the current and envisioned applications of AO in clinical practice. Raw individual Adaptive-Optics-corrected flood-illuminated retinal images are usually quite noisy because of safety flux limitations. These flood-illuminated images are also of poor contrast. Interpretation of such images is therefore difficult without an appropriate post-processing, which typically includes the registration of the recorded image stack into a mosaic image and the restoration of the latter. This processing can be used both for direct interpretation by a physician and for further automatic processing [1].

We have developed a novel image registration method in a MAP framework, based on previous work in astronomical imaging [2], and tailored for the specifics of retinal imaging [3], more precisely to the fact that the illumination of the retina and the transmission of the instrument is quite non-homogeneous, which makes conventional registration algorithm likely to fail (see [4, 5] for reviews on existing registration methods).

The obtained mosaic image must then be deconvolved in order to visually restore the high-resolution brought by adaptive optics. Indeed, flood-illuminated images are of poor contrast due to the three-dimensional nature of retinal imaging, meaning that the image contains information coming from both the in-focus plane and the out-of-focus planes of the object. This deconvolution is difficult for two reasons. Firstly because the point spread function (PSF) is not well known, a problem known as myopic deconvolution. Secondly because we are imaging a 3D object with a 2D imager.

We have developed an image model for dealing with the latter fact, resulting in the recorded 2D image being a convolution of an invariant 2D object with an unknown linear combination of 2D PSFs. We address this problem by means of an unsupervised myopic deconvolution.

In this communication we show results of the whole processing chain (image registration followed by unsupervised myopic deconvolution) on experimental retinal images.

2. RETINAL IMAGE REGISTRATION

2.1. Imaging model and registration method

We model each image z_j acquired by the retinal camera, at every pixel (k, l), as a shifted portion of the reference image i, multiplied by the illumination+transmission map (hereafter global transmission) c and corrupted by noise :

$$z_j(k,l) = c(k,l) \times [i \star \delta(x_j, y_j)]_{(k,l)} + n(k,l), \qquad (1)$$

where c is the uneven global transmission, i is the reference image, $\star$ is the convolution operator, (x_j, y_j) is the shift of the $j-$th image z_j, $\delta(x_j, y_j)$ is a Dirac distribution centered at (x_j, y_j), [.] is the sampling operator at pixel (k, l) and n is the measurement noise.

In this imaging modality, noise is a mixture of readout noise, which is homogeneous white Gaussian, and of photonic noise, which follows Poisson statistics. This mixture can reasonably be approximated as inhomogeneous white Gaussian [7].The total noise variance is parameterized as the inverse of a weight map $w_j(k, l)$, which allows us to be able to cope with dead pixels simply by setting a null weight for these pixels.

c can be estimated by averaging a large enough (> 20) number of individual images z_j or as the linear combination of base vectors (*e.g.* Zernike polynomials or other low-order polynomials).

In order to avoid uncontrolled noise amplification in regions of the reference image that have not been recorded, or recorded with a very low SNR, we use the following prior : we assume that the reference image follow *a priori* a white Gaussian statistics with a mean value i_0 and a variance $1/w_r(k, l)$. In practice we often take $w_r(k, l) = \mu \langle w_j(k, l) \rangle_j$, where μ is a hyperparameter allowing us to tune the regularization.

We want to jointly estimate the reference image $i(k, l)$ and the shifts x_j, y_j, with a prior on the reference image. We do so in a Bayesian framework by a Maximum *A Posteriori* estimation. The MAP criterion to be minimized reads :

$$\begin{aligned} L(i, \{x_j, y_j\}) &= \sum_{j=1}^{N} \sum_{k,l} w_j(k, l).|z_j(k, l) - \\ & \quad c(k, l) \times [i \star \delta(x_j, y_j)]_{(k,l)}|^2 \qquad (2) \\ &+ \sum_{k,l} w_r(k, l).|i(k, l) - i_0(k, l)|^2 \end{aligned}$$

By cancelling the derivative of $L(i, \{x_j, y_j\})$ with respect to the reference image, we obtain an analytical expression of the reference image $\hat{i}$ that minimizes the criterion for a given set of shifts $\{x_j, y_j\}$:

$$\hat{i}(k, l; \{x_j, y_j\}) = \frac{w_r(k, l).i_0(k, l) + \sum_{j=1}^{N} (w_j i_j c)(k + x_j, l + y_j)}{w_r(k, l) + \sum_{j=1}^{N} (w_j c^2)(k + x_j, l + y_j)}. \qquad (3)$$

If we substitute the analytical expression of $\hat{i}(k, l; \{x_j, y_j\})$ in Eq. (2), we obtain a new criterion $L'(\{x_j, y_j\})$ that only depends on the shifts $\{x_j, y_j\}$. Once the criterion is minimized (using, for example, the VMLM-B method or a conjugate-gradient method), the reference image is computed using Eq. (3).

2.2. Results

40 images acquired with the Paris Quinze-Vingts Hospital AO Fundus Camera (RTX-1 by Imagine Eyes, Orsay, France) were registered using the MAP registration method. Figure 1 shows 1 of the 20 images acquired, Fig 2 shows the estimated global transmission, and Figure 3 shows the estimated reference image. The expansion of the field of view is clearly visible as well as the improvement in contrast of the photoreceptors. Thanks to the regularization, there is no visible noise amplification in the areas of the individual images where the SNR was low (the dark areas in the mosaic).

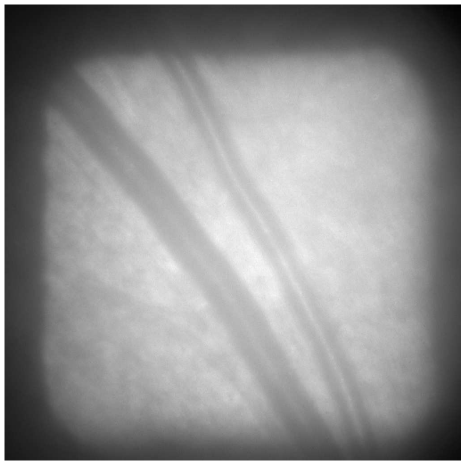

Fig. 1. 1 of the 40 individual images.

Fig. 2. Estimated global transmission.

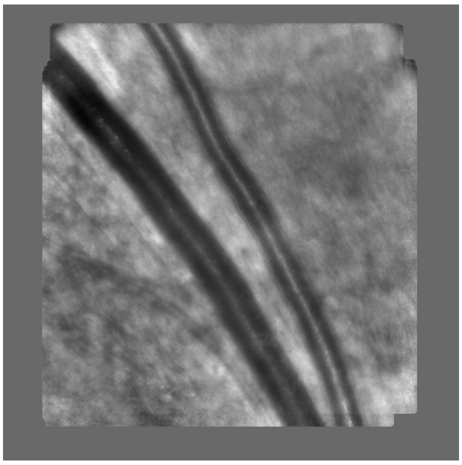

Fig. 3. Estimated mosaic using 20 individual images

3. MYOPIC DECONVOLUTION

3.1. Imaging model

The object and the imaging process are both three-dimensional (3D). If we recorded a stack $i_{3\mathrm{D}}$ of 2D images focused at different depths in the object, a reasonable image formation model, after background subtraction, could be written as a 3D convolution :

$$\mathbf{i}_{3\mathrm{D}} = \mathbf{h}_{3\mathrm{D}} *_{3\mathrm{D}} \mathbf{o}_{3\mathrm{D}} + \mathbf{n}, \tag{4}$$

where $\mathbf{i}_{3\mathrm{D}}$ is the 3D image, $\mathbf{o}_{3\mathrm{D}}$ is the 3D object, $*_{3\mathrm{D}}$ denotes the 3D convolution operator, $\mathbf{h}_{3\mathrm{D}}$ is the 3D PSF and $\mathbf{n}$ is the noise. In practice, we only record one slice of such a 3D image. Therefore, in order to cope with the lack of information, we assume that our object is shift invariant along the optical axis :

$$o_{3\mathrm{D}}(x, y, z) = o_{2\mathrm{D}}(x, y)\, \alpha(z), \tag{5}$$

where $\alpha(z)$ is the normalized flux emitted by the plane at depth z ($\int \alpha(z)\mathrm{d}z = 1$).

In practice this invariance must only be verified over the depth of focus of the instrument (50 microns for an AO flood imager, $10-15$ microns for a confocal imager).

With this assumption, the imaging model reads :

$$i(x, y) = (h_{2\mathrm{D}} *_{2\mathrm{D}} o_{2\mathrm{D}})(x, y) + n(x, y)\,, \tag{6}$$

with $h_{2\mathrm{D}}$ an *effective* 2D PSF which depends on the longitudinal brightness distribution of the object $\alpha(z)$ and on the 3D PSF :

$$h_{2\mathrm{D}}(x, y) = \int \alpha(-z)\, h_{3\mathrm{D}}(x, y, z)\, \mathrm{d}z.$$

The 2D image $i(x, y)$ at the focal plane of the instrument is the 2D convolution of a 2D object and a global PSF h which is the linear combination of the individual 2D PSFs (each one conjugated with a different plane of the object) weighted by the flux back-scattered from each plane.

After discretization and using Riemann sum to approximate the integral :

$$h_{2\mathrm{D}}(x, y) \approx \sum_j \alpha_j\, h_j(x, y)\,, \tag{7}$$

with $h_j(x, y) \triangleq h_{3\mathrm{D}}(x, y, z_j)$ the 2D lateral PSF at depth z_j and $\alpha_j = \alpha(z_j)\, \Delta z_j$ where Δz_j is the effective thickness of the jth layer. We define $\boldsymbol{\alpha} = \{\alpha_j\}_j$ as the vector of unknowns that parameterize the PSF. α is normalized ($\sum \alpha_j = 1$) and each parameter is positive ($\alpha_j \geq 0$). We search for $h_{2\mathrm{D}}$ as a linear combination of a basis of PSF's, each corresponding to a given plane.

In the following, we consider short-exposure diffractive PSF's so that each h_j can be computed from the residual aberrations measured with a WFS and the knowledge of the defocus of plane z_j.

3.2. Unsupervised marginal estimation of the PSF

Joint estimation of the object and the PSF fails even for a small number of unknowns because of a degeneracy of the joint MAP criterion [8]. The estimator proposed is the marginal estimator, which has better properties [9], already proposed in the literature in other contexts including estimation of aberrations by use of phase diversity [10]. The principle of marginal estimation is to integrate the object $\mathbf{o}$ out of the problem (*i.e.*, marginalize the posterior likelihood [11]). We integrate the joint probability of the object $\mathbf{o}$ and the PSF parameters $\boldsymbol{\alpha}$ over all the possible values of object $\mathbf{o}$.

$$\hat{\boldsymbol{\alpha}} = \arg\max_{\alpha} \int p(\mathbf{i}, \mathbf{o}, \boldsymbol{\alpha}; \theta)\mathrm{d}\mathbf{o}. \tag{8}$$

Marginalization drastically reduces the number of unknowns to be retrieved, from the total number of pixels of the image + the PSF parameters in the joint estimation case to just a few PSF parameters. It gives us a true maximum likelihood or maximum a posteriori (depending on the prior on the estimated parameters) estimator of the parameters of interest, namely, the PSF parameters. After estimation of the PSF parameters $\boldsymbol{\alpha}$, the object is restored, for instance, by Wiener filtering of the image with the estimated global PSF and hyperparameters.

$$\hat{\boldsymbol{\alpha}}_{\mathrm{ML}} = \arg\max_{\alpha} p(\mathbf{i}, \boldsymbol{\alpha}; \boldsymbol{\theta}) = \arg\max_{\alpha} p(\mathbf{i}|\boldsymbol{\alpha}; \boldsymbol{\theta})p(\boldsymbol{\alpha}; \boldsymbol{\theta}). \tag{9}$$

AO retinal images are dominated by a strong and quite homogeneous background. In the following, we will therefore assume that the noise is homogeneous white Gaussian with a variance σ^2. For the object, we choose a homogeneous Gaussian prior probability distribution with a mean value $\mathbf{o}_{\mathrm{m}}$ and a covariance matrix $\mathbf{R}_{\mathrm{o}}$.

With a circulant approximation, the marginal criterion can be written in the Fourier domain as follows :

$$J_{\mathrm{ML}}(\boldsymbol{\alpha}) = \frac{1}{2}\sum_{\nu} \ln S_{\mathrm{o}}(\nu) + \frac{1}{2}\sum_{\nu} \ln\left(|\tilde{h}(\nu)|^2 + \frac{S_{\mathrm{n}}}{S_{\mathrm{o}}(\nu)}\right)$$
$$+\frac{1}{2}\sum_{\nu} \frac{1}{S_{\mathrm{o}}(\nu)} \frac{|\tilde{i}(\nu) - \tilde{h}(\nu)\tilde{o}_{\mathrm{m}}(\nu)|^2}{|\tilde{h}(\nu)|^2 + \frac{S_{\mathrm{n}}}{S_{\mathrm{o}}(\nu)}} + B', \tag{10}$$

where S_{n} is the constant noise power spectral density (PSD), S_{o} is the object PSD, ν is the spatial frequency and $\tilde{x}$ denotes the two-dimensional Fast Fourier Transform of x.

The marginal estimator allows us to estimate the set of hyperparameters θ (actually the object PSD S_{o} and noise PSD S_{n}) together with the PSF coefficients in an automatic manner. This method is called unsupervised estimation.

In order to reduce the number of hyperparameters we must estimate, we choose to model the object PSD S_{o} with the 3-parameter model of [12]. There is no analytical expression for the minimum value of the criterion so the minimization has to be done numerically. In our case, the minimization is performed with a Variable Metric with Limited Memory, Bounded (VMLM-B) [13].

Figure 4 shows, on simulated data, the RMS error on estimation of the PSF coefficients for different values of noise and a varying data size, both in the supervised and unsupervised cases. For a given data size, both in the supervised and in the unsupervised estimation, the marginal estimator RMS error tends towards zero (*i.e.*, the estimated parameters $\boldsymbol{\alpha}$ tends towards the exact value) when noise decreases. Even more interestingly, for a given noise value, error tends towards zero as the size of data increases. For example, for a 128×128 pixel image and for noise $\sigma = 5\%$ of the max value of the image, the RMS error on the PSF coefficient α estimation is less than 3%. This simulation shows that the unsupervised marginal estimator exhibits, in practice, its appealing theoretical properties, which opens the way to its use on experimental images.

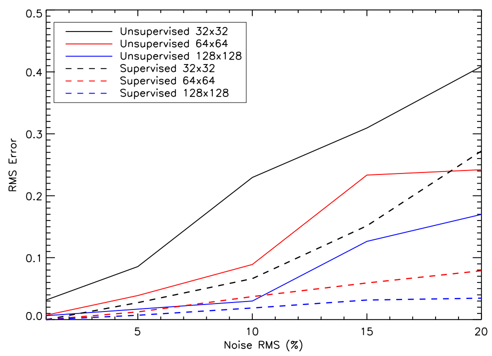

Fig. 4. RMS error on the estimation of the PSF as a function of noise level and image size

3.3. Experimental results

The mosaic image of figure 3 was deconvolved using the marginal estimator. The estimated object is shown in figure 5.

The vessel features of are much more clearly visible on the estimated object than on the registered mosaic. In particular the contrast of the blood vessel walls is significantly improved, allowing for an easier measurement of their width.

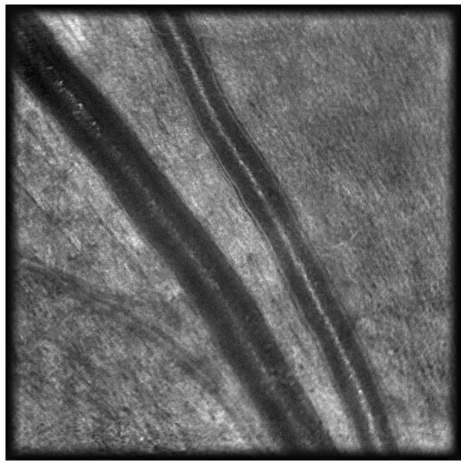

Fig. 5. Estimated object after marginal estimation of the PSF.

4. CONCLUSION

We have developed a complete processing chain for AO-corrected flood-illuminated retinal images, which first performs a joint registration of all raw images into a mosaic with improved contrast and SNR, and then deconvolves this mosaic in a myopic and unsupervised fashion. The image registration uses a physics-based imaging model that takes into account the illumination inhomogeneity and uses all the images jointly, in order to make the registration more robust than common pair-wise intensity-based registration methods. The deconvolution method explicitly models the fact that the object being imaged is three-dimensional. With an appropriate simplifying assumption on the object structure, the deconvolution boils down to a 2D deconvolution where both the object and the PSF are unknown. This problem is addressed satisfactorily by a marginal estimation of the PSF followed by a classical deconvolution. The deconvolution method additionally estimates the hyper-parameters in an unsupervised way, so as to be usable by non-specialists. This registration and deconvolution chain has been successfully applied to experimental *in vivo* images of human photoreceptors (not shown here for lack of space) and of human retinal vessels.

5. REFERENCES

[1] M. Pâques, F. Rossant, N. Lermé, C. Miloudi, C. Kulcsar, J. Sahel, L. Mugnier, I. Bloch, and E. Kock, "Adaptive optics imaging of retinal microstructures," in *International Workshop on Computational Intelligence for Multimedia Understanding*, 2014.

[2] D. Gratadour, L. M. Mugnier, and D. Rouan, "Sub-pixel image registration with a maximum likelihood estimator," *Astron. Astrophys.*, vol. 443, pp. 357–365, Nov. 2005.

[3] L. Mugnier and L. Blanco, "Procédé d'estimation de l'image totale d'une scène," Brevet Onera-Cnrs, Déposé le 26 juin 2013, Numéro d'enregistrement 13.56129.

[4] Lisa Gottesfeld Brown, "A survey of image registration techniques," *ACM Comput. Surv.*, vol. 24, no. 4, pp. 325–376, Dec. 1992.

[5] Barbara Zitova and Jan Flusser, "Image registration methods : a survey," *Image and Vision Computing*, vol. 21, pp. 977–1000, 2003.

[6] L. Blanco and L. M. Mugnier, "Marginal blind deconvolution of adaptive optics retinal images," *Opt. Express*, vol. 19, no. 23, pp. 23227–23239, Nov. 2011.

[7] L. M. Mugnier, T. Fusco, and J.-M. Conan, "MISTRAL : a myopic edge-preserving image restoration method, with application to astronomical adaptive-optics-corrected long-exposure images.," *J. Opt. Soc. Am. A*, vol. 21, no. 10, pp. 1841–1854, Oct. 2004.

[8] L. Blanco and L. M. Mugnier, "Marginal blind deconvolution of adaptive optics retinal images," *Opt. Express*, vol. 19, no. 23, pp. 23227–23239, Nov 2011.

[9] E. Lehmann, *Theory of point estimation*, John Wiley, New York, NY, 1983.

[10] Amandine Blanc, Laurent M. Mugnier, and Jérôme Idier, "Marginal estimation of aberrations and image restoration by use of phase diversity," *J. Opt. Soc. Am. A*, vol. 20, no. 6, pp. 1035–1045, Jun 2003.

[11] L. Blanc-Féraud, L. Mugnier, and A. Jalobeanu, "Blind image deconvolution," in *Inverse Problems in Vision and 3D Tomography*, Ali Mohammad-Djafari, Ed., chapter 3, pp. 97–121. ISTE / John Wiley, London, 2010.

[12] J.-M. Conan, L. M. Mugnier, T. Fusco, V. Michau, and G. Rousset, "Myopic deconvolution of adaptive optics images by use of object and point spread function power spectra," *Appl. Opt.*, vol. 37, no. 21, pp. 4614–4622, July 1998.

[13] É. Thiébaut, "Optimization issues in blind deconvolution algorithms," in *Astronomical Data Analysis II*, J.-L. Starck and F. D. Murtagh, Eds. Proc. Soc. Photo-Opt. Instrum. Eng., Dec. 2002, vol. 4847, pp. 174–183.